IFAC 2011 World Congress, Milan, Italy, 28 August - 2 September 2011.

# Complex Dynamic Models of Multi-phase Permanent Magnet Synchronous Motors

**R. Zanasi** *, **F. Grossi** *, **M. Fei** *

* *Information Engineering Department, University of Modena and Reggio Emilia, Via Vignolese 905, 41100 Modena, Italy,*
*e-mail:* {roberto.zanasi, federica.grossi, marco.fei}@unimore.it.

Abstract: In the paper two power-invariant real and complex state space transformations for modeling multi-phase electrical machines in a compact and general form are proposed. In particular the paper deals with the modeling of multi-phase permanent magnet synchronous machines with an arbitrary number of phases and an arbitrary shape of the rotor flux. The dynamic model of the motor is obtained using a Lagrangian approach and in the frame of the Power-Oriented Graphs technique. The obtained models are equivalent from a mathematical point of view and can be directly implemented in Simulink. The complex transformed model is quite compact and uses a reduced order state vector. Some simulation results end the paper.

*Keywords:* Dynamic Modeling, Multi-phase synchronous motor, Power-Oriented Graphs, State space transformation.

## 1. INTRODUCTION

In the literature many coordinate transformations have been proposed in order to write the dynamic equations of synchronous electric motors in a proper form. The transformations typically used are the Park, the Clarke and Fortescue transformations, see Clarke (1950), Park (1929) and Fortescue (1918), respectively. Usually these transformations are exploited for three-phase machines, see Paap (2000), but they can be extended to the case of multi-phase machines, where the number of phases is greater than three. The extended Park and Clarke transformations are based on a real matrix (see Parsa and Toliyat (2005) and Kestelyn et al. (2002)), the Fortescue transformation is based on a complex matrix which contains complex vectors and their complex conjugate (see White and Woodson (1959)) while in the space vector approach (see Grandi et al. (2006)) only one half of the Fortescue matrix is considered (i.e. without the complex conjugate part). Unfortunately, all these transformations *are not power invariant*, i.e. after the transformations the power flows cannot be expressed as the simple product of the transformed coniugate power variables, but always a correction coefficient must be used.
In this paper two power invariant state-space transformations (one real and one complex) for modeling multi-phase synchronous machines are proposed. They are suitable for machines with an arbitrary odd number of stator phases and for an arbitrary shape of the rotor flux. Using the proposed transformations one obtains the dynamics of the system written in a very simple and compact form, without the need of considering a set of separate fictitious 2-phase machines as it is usually done in the literature (see, for example, Semail et al. (2004)).
In this paper the dynamic model of multi-phase synchronous motors, usually obtained by means of classical mathematical methods is obtained using a Lagrangian approach (see Zanasi and Grossi (2008)) in the frame of the Power-Oriented Graphs (POG) technique. This graphical modeling technique shows the power flows within the system, allows to write the state space equations of the system in a very compact form with a vectorial notation and provides a dynamic model that can be directly implemented in Simulink.
The paper is organized as follows. Sec. 2 introduces the main features of POG technique. Sec. 3 shows the details of the POG dynamic model of the multi-phase synchronous motors, introduces the two proposed state space transformations and shows the obtained transformed systems. Some simulation results are presented in Sec. 4 and conclusions are given in Sec. 5.

## 2. POWER-ORIENTED GRAPHS BASIC PRINCIPLES

The Power-Oriented Graphs technique, see Zanasi (1991) and Zanasi (2010), is an energy-based technique suitable for modeling physical systems. The POG are block diagrams combined with a particular modular structure essentially based on the use of the two blocks shown in Fig. 1.a and Fig. 1.b: the *elaboration block* (e.b.) stores and/or dissipates energy (i.e. springs, masses, dampers, capacities, inductances, resistances, etc.), the *connection block* (c.b.) redistributes the power within the system

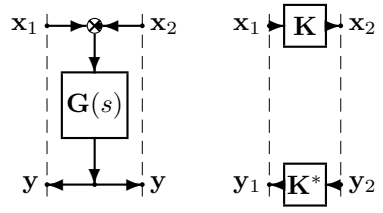


a) *e. b.* b) *c. b.*

Figure 1. POG basic blocks: a) *elaboration block*; b) *connection block*.

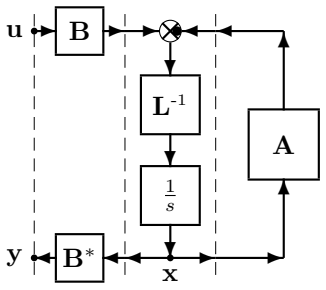


$$\begin{cases} \mathbf{L}\,\dot{\mathbf{x}} = -\mathbf{A}\mathbf{x} + \mathbf{B}\mathbf{u} \\ \mathbf{y} = \mathbf{B}^*\mathbf{x} \end{cases} \quad (1)$$

$$\Downarrow (\mathbf{x} = \mathbf{T}\mathbf{z})$$

$$\begin{cases} \overline{\mathbf{L}}\dot{\mathbf{z}} = -\overline{\mathbf{A}}\mathbf{z} + \overline{\mathbf{B}}\mathbf{u} \\ \mathbf{y} = \overline{\mathbf{B}}^*\mathbf{z} \end{cases} \quad (2)$$

Figure 2. POG scheme of a generic dynamic system in the complex domain.

without storing nor dissipating energy (i.e. any type of gear reduction, transformers, etc.). The c.b. transforms the power variables with the constraint $\mathbf{x}_1^*\mathbf{y}_1 = \mathbf{x}_2^*\mathbf{y}_2$. The circle in the e.b. is a summation element and the black spot represents a minus sign that multiplies the entering variable. The POG keep a direct correspondence between the dashed sections of the graphs and real power sections of the modeled system: the scalar product $\mathbf{x}^*\mathbf{y}$ of the two *power vectors* $\mathbf{x}$ and $\mathbf{y}$ involved in each dashed line of a POG, see Fig. 1, has the physical meaning of *the power flowing through that particular section*. Another important aspect of the POG technique is the direct correspondence between the POG representations and the corresponding state space descriptions. For example, the POG scheme shown in Fig. 2 can be represented by the state space equations given in (1) where the *energy matrix* $\mathbf{L}$ is symmetric and positive definite: $\mathbf{L} = \mathbf{L}^* > 0$. For such a system, the stored energy $E_s$ and the dissipating power $P_d$ can always be expressed as follows: $E_s = \frac{1}{2}\mathbf{x}^*\mathbf{L}\,\mathbf{x}$, $P_d = \mathbf{x}^*\mathbf{A}\,\mathbf{x}$. The dynamic model (1) can be transformed and reduced to system (2) using a "congruent" transformation $\mathbf{x} = \mathbf{T}\mathbf{z}$ (matrix $\mathbf{T}$ can also be rectangular and time-varying) where $\overline{\mathbf{L}} = \mathbf{T}^*\mathbf{L}\mathbf{T}$, $\overline{\mathbf{A}} = \mathbf{T}^*\mathbf{A}\mathbf{T} + \mathbf{T}^*\mathbf{L}\dot{\mathbf{T}}$ and $\overline{\mathbf{B}} = \mathbf{T}^*\mathbf{B}$.

### *2.1 Notations*

The full and diagonal matrices will be denoted as follows:

$$\overset{i}{\underset{1:n}{\big|\big[}}\, R_{i,j} \,\overset{j}{\underset{1:m}{\big]\big|}} = \begin{bmatrix} R_{11} & R_{12} & \cdots & R_{1m} \\ R_{21} & R_{22} & \cdots & R_{2m} \\ \vdots & \vdots & \ddots & \vdots \\ R_{n1} & R_{n2} & \cdots & R_{nm} \end{bmatrix}, \quad \overset{i}{\underset{1:n}{\big|\big[}}\, R_i \,\big]\big| = \begin{bmatrix} R_1 & & & \\ & R_2 & & \\ & & \ddots & \\ & & & R_n \end{bmatrix}$$

The symbols $\overset{i}{\underset{1:n}{\big|\big[}}\, R_i \,\big]\big|$ and $\big|\big[\, R_i \,\overset{i}{\underset{1:n}{\big]\big|}}$ will denote the column and row matrices. The symbol $\sum_{n=a:d}^{b} c_n = c_a + c_{a+d} + c_{a+2d} + \ldots$ will be used to represent the sum of a succession of numbers $c_n$ where the index $n$ ranges from $a$ to $b$ with increment $d$, that is, using the Matlab symbology, $n = [a : d : b]$. Using the previous notations one can represent, for example, the following matrix:

$$\overset{i}{\underset{1:2:6}{\big|\big[}}\, R_{i,j} \,\overset{j}{\underset{3:3:11}{\big]\big|}} = \begin{bmatrix} R_{13} & R_{16} & R_{19} \\ R_{33} & R_{36} & R_{39} \\ R_{53} & R_{56} & R_{59} \end{bmatrix}$$

Given a complex matrix $\mathbf{A}$, the conjugate matrix will be denoted by $\mathbf{A}^\circ$, the transpose matrix by $\mathbf{A}^{\mathrm{T}}$ and the conjugate transpose matrix by $\mathbf{A}^*$. The following relations hold: $\mathbf{A}^* = (\mathbf{A}^\circ)^{\mathrm{T}} = (\mathbf{A}^{\mathrm{T}})^\circ$. The symbol $\mathbf{0}$ will be used to represent a zero block matrix of proper dimensions.

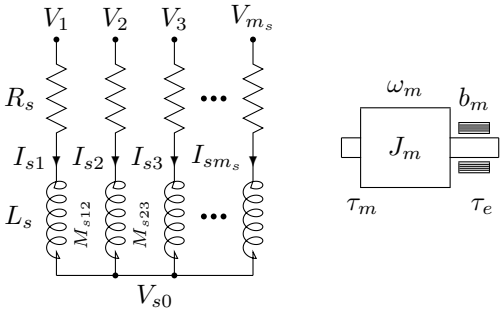


Figure 3. Basic structure of a multi-phase synchronous motor.

| | |
|---|---|
| $m_s$ | number of motor phases |
| $p$ | number of polar expansions |
| $\theta$, $\theta_m$ | electric and rotor angular positions: $\theta = p\,\theta_m$ |
| $\omega$, $\omega_m$ | electric and rotor angular velocities: $\omega = p\,\omega_m$ |
| $R_s$ | $i$-th stator phase resistance |
| $L_s$ | $i$-th stator phase self induction coefficient |
| $M_{s0}$ | maximum value of mutual inductance between stator phases |
| $\phi_c(\theta)$ | total rotor flux chained with stator phase 1 |
| $\varphi_c$ | maximum value of function $\phi_c(\theta)$ |
| $J_m$ | rotor moment of inertia |
| $b_m$ | rotor linear friction coefficient |
| $\tau_m$ | electromotive torque acting on the rotor |
| $\tau_e$ | external load torque acting on the rotor |
| $\gamma_s$ | basic angular displacement ($\gamma_s = 2\pi/m_s$) |

Table 1. Parameters of the multi-phase synchronous motor.

## 3. ELECTRICAL MOTORS MODELLING

The basic structure of a permanent magnet synchronous motor with an *odd* number $m_s$ of star-connected phases is shown in Fig. 3. The parameters of the considered system are shown in Tab. 1. Let ${}^t\mathbf{I}_s$ and ${}^t\mathbf{V}_s$ denote the following current and voltage stator vectors:

$${}^t\mathbf{I}_s = [I_{s1}\ I_{s2}\ \cdots\ I_{sm_s}]^{\mathrm{T}}, \quad {}^t\mathbf{V}_s = [V_{s1}\ V_{s2}\ \cdots\ V_{sm_s}]^{\mathrm{T}}. \quad (3)$$

Using a "Lagrangian" approach, see Zanasi and Grossi (2008) and Zanasi and Grossi (2009), the dynamic equations $S_t$ of the considered electric motor expressed with respect to the external fixed frame $\Sigma_t$ are:

$$\left[\begin{array}{c|c} {}^t\mathbf{L}_s & \mathbf{0} \\ \hline \mathbf{0} & J_m \end{array}\right]\left[\begin{array}{c} {}^t\dot{\mathbf{I}}_s \\ \hline \dot{\omega}_m \end{array}\right] = -\left[\begin{array}{c|c} {}^t\mathbf{R}_s & {}^t\mathbf{K}_\tau(\theta) \\ \hline -{}^t\mathbf{K}_\tau^{\mathrm{T}}(\theta) & b_m \end{array}\right]\left[\begin{array}{c} {}^t\mathbf{I}_s \\ \hline \omega_m \end{array}\right] + \left[\begin{array}{c} {}^t\mathbf{V}_s \\ \hline -\tau_e \end{array}\right] \quad (4)$$

These equations, in the literature, are usually rewritten and transformed using the Park and Fortescue transformations, see White and Woodson (1959). The *Park transformation*, also known as $dq0$ transformation, is based on the following matrix:

$${}^t\widehat{\mathbf{T}}_P = \frac{2}{m_s} \overset{h}{\underset{0:m_s-1}{\Big|\Big[}}\, \cos(k(\theta - h\gamma_s)) \ \ \sin(k(\theta - h\gamma_s)) \,\overset{k}{\underset{1:2:m_s-2}{\Big]\Big|}}$$

$$= \frac{2}{5}\begin{bmatrix} \cos(\theta) & \sin(\theta) & \cos(3\theta) & \sin(3\theta) \\ \cos(\theta-\gamma_s) & \sin(\theta-\gamma_s) & \cos(3\theta-3\gamma_s) & \sin(3\theta-3\gamma_s) \\ \cos(\theta-2\gamma_s) & \sin(\theta-2\gamma_s) & \cos(3\theta-6\gamma_s) & \sin(3\theta-6\gamma_s) \\ \cos(\theta-3\gamma_s) & \sin(\theta-3\gamma_s) & \cos(3\theta-9\gamma_s) & \sin(3\theta-9\gamma_s) \\ \cos(\theta-4\gamma_s) & \sin(\theta-4\gamma_s) & \cos(3\theta-12\gamma_s) & \sin(3\theta-12\gamma_s) \end{bmatrix}_{m_s=5}$$

and the *Fortescue transformation*, also known as symmetrical transformation, is based on the following matrix:

$$ {}^{t}\widehat{\mathbf{T}}_F = \frac{1}{m_s} \Big\|\!\Big[ e^{j\,h\,k\,\gamma_s} \Big]\!\Big\|_{0:m_s-1 \quad 0:m_s-1}^{h \quad k} = \frac{1}{5} \begin{bmatrix} 1 & 1 & 1 & 1 & 1 \\ 1 & e^{j\gamma_s} & e^{j2\gamma_s} & e^{j3\gamma_s} & e^{j4\gamma_s} \\ 1 & e^{j2\gamma_s} & e^{j4\gamma_s} & e^{j6\gamma_s} & e^{j8\gamma_s} \\ 1 & e^{j3\gamma_s} & e^{j6\gamma_s} & e^{j9\gamma_s} & e^{j12\gamma_s} \\ 1 & e^{j4\gamma_s} & e^{j8\gamma_s} & e^{j12\gamma_s} & e^{j16\gamma_s} \end{bmatrix}_{m_s=5} $$

In Grandi et al. (2006) the complex conjugate terms of Fortescue's transformation are neglected in order to reduce the number of the dynamic equations. The main drawback of these transformations is that they *are not power invariant*. In the following two power-invariant transformations are proposed.

### *3.1 System $S_\omega$ in the rotating frame $\Sigma_\omega$*

Using the POG approach and applying to system $S_t$ in (4) the following transformation matrix:

$$ {}^{t}\mathbf{T}_\omega = \sqrt{\frac{2}{m_s}} \Big\|\!\Big[ \cos(k(h\gamma_s - \theta)) \;,\; \sin(k(h\gamma_s - \theta)) \Big]\!\Big\|_{0:m_s-1 \quad 1:2:m_s-2}^{h \quad k} \quad (5) $$

one obtains a transformed and reduced system $S_\omega$ described by real variables:

$$ \left[\begin{array}{c|c} {}^{\omega}\mathbf{L}_s & \mathbf{0} \\ \hline \mathbf{0} & J_m \end{array}\right] \left[\begin{array}{c} {}^{\omega}\dot{\mathbf{I}}_s \\ \hline \dot{\omega}_m \end{array}\right] = - \left[\begin{array}{c|c} {}^{\omega}\mathbf{R}_s + {}^{\omega}\mathbf{L}_s\,{}^{\omega}\mathbf{J}_s & {}^{\omega}\mathbf{K}_\tau(\theta) \\ \hline -\,{}^{\omega}\mathbf{K}_\tau^{\mathrm{T}}(\theta) & b_m \end{array}\right] \left[\begin{array}{c} {}^{\omega}\mathbf{I}_s \\ \hline \omega_m \end{array}\right] + \left[\begin{array}{c} {}^{\omega}\mathbf{V}_s \\ \hline -\tau_e \end{array}\right] \quad (6) $$

where ${}^{\omega}\mathbf{I}_s = {}^{t}\mathbf{T}_\omega^{\mathrm{T}}\,{}^{t}\mathbf{I}_s$, ${}^{\omega}\mathbf{L}_s = {}^{t}\mathbf{T}_\omega^{\mathrm{T}}\,{}^{t}\mathbf{L}_s\,{}^{t}\mathbf{T}_\omega$, ${}^{\omega}\mathbf{R}_s = {}^{t}\mathbf{T}_\omega^{\mathrm{T}}\,{}^{t}\mathbf{R}_s\,{}^{t}\mathbf{T}_\omega = {}^{t}\mathbf{R}_s$, ${}^{\omega}\mathbf{J}_s = {}^{t}\mathbf{T}_\omega^{\mathrm{T}}\,{}^{t}\dot{\mathbf{T}}_\omega$, ${}^{\omega}\mathbf{K}_\tau = {}^{t}\mathbf{T}_\omega^{\mathrm{T}}\,{}^{t}\mathbf{K}_\tau$ and ${}^{\omega}\mathbf{V}_s = {}^{t}\mathbf{T}_\omega^{\mathrm{T}}\,{}^{t}\mathbf{V}_s$. Matrix ${}^{t}\mathbf{T}_\omega(\theta)$ is a function of the electrical angle $\theta$ and transforms the system variables from the original reference frame $\Sigma_t$ to a transformed rotating frame $\Sigma_\omega$. For $m_s = 5$ the transformation matrix ${}^{t}\mathbf{T}_\omega$ has the following form:

$$ {}^{t}\mathbf{T}_\omega = \sqrt{\frac{2}{5}} \begin{bmatrix} \cos(-\theta) & \sin(-\theta) & \cos(-3\theta) & \sin(-3\theta) \\ \cos(\gamma_s-\theta) & \sin(\gamma_s-\theta) & \cos(3\gamma_s-3\theta) & \sin(3\gamma_s-3\theta) \\ \cos(2\gamma_s-\theta) & \sin(2\gamma_s-\theta) & \cos(6\gamma_s-3\theta) & \sin(6\gamma_s-3\theta) \\ \cos(3\gamma_s-\theta) & \sin(3\gamma_s-\theta) & \cos(9\gamma_s-3\theta) & \sin(9\gamma_s-3\theta) \\ \cos(4\gamma_s-\theta) & \sin(4\gamma_s-\theta) & \cos(12\gamma_s-3\theta) & \sin(12\gamma_s-3\theta) \end{bmatrix}_{m_s=5}. $$

The POG block scheme of a multi-phase synchronous motor (6) in the transformed rotating frame $\Sigma_\omega$ is shown in Fig. 4. The POG scheme clearly puts in evidence five different power sections. The *connection block* between sections ①-② represents the state space transformation ${}^{t}\mathbf{T}_\omega$ between the fixed reference frame $\Sigma_t$ and the rotating reference frame $\Sigma_\omega$. The *elaboration blocks* present between the power sections ②-③ represent the *Electrical part* of the system, while the blocks present between sections ④-⑤ represent the *Mechanical part* of the system. The *connection block* present between sections ③-④ represents the energy and power conversion (without accumulation nor dissipation) between the electrical and mechanical parts of the motor. Let $p(t) = {}^{t}\mathbf{V}_s^T\,{}^{t}\mathbf{I}_s$ and $s(t) = {}^{\omega}\mathbf{V}_s^T\,{}^{\omega}\mathbf{I}_s$ denote the instantaneous powers in sections ① and ② of the POG scheme in Fig. 4. It can be easily proved that the transformation ${}^{t}\mathbf{T}_\omega$ *is power-invariant*, indeed the power $p(t)$ in section ① is equal to the power $s(t)$ in section ②:

$$ p(t) = {}^{t}\mathbf{V}_s^T\,{}^{t}\mathbf{I}_s = {}^{\omega}\mathbf{V}_s^T\,{}^{t}\mathbf{T}_\omega^T\,{}^{t}\mathbf{T}_\omega\,{}^{\omega}\mathbf{I}_s = {}^{\omega}\mathbf{V}_s^T\,{}^{\omega}\mathbf{I}_s = s(t). $$

The square matrices ${}^{\omega}\mathbf{L}_s$, ${}^{\omega}\mathbf{J}_s$ and ${}^{\omega}\mathbf{R}_s$ are defined as:

$$ {}^{\omega}\mathbf{L}_s = \Big\|\!\Big[ \begin{smallmatrix} L_{sk} & 0 \\ 0 & L_{sk} \end{smallmatrix} \Big]\!\Big\|_{1:2:m_s-2}^{k}, \quad {}^{\omega}\mathbf{J}_s = \Big\|\!\Big[ \begin{smallmatrix} 0 & -k\,\omega \\ k\,\omega & 0 \end{smallmatrix} \Big]\!\Big\|_{1:2:m_s-2}^{k}, \quad {}^{\omega}\mathbf{R}_s = \Big\|\!\Big[ R_s \Big]\!\Big\|_{1:m_s-1}^{i} $$

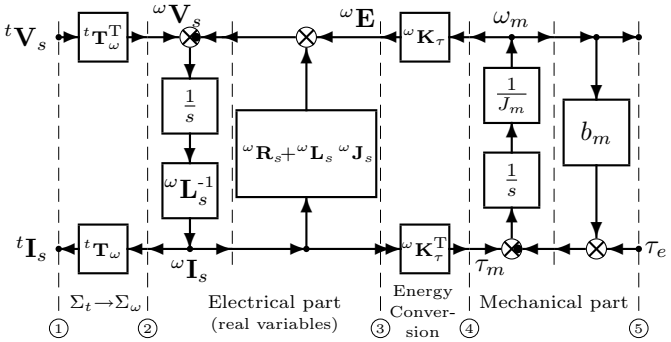


Figure 4. POG block scheme of a multi-phase synchronous motor in the rotating frame $\Sigma_\omega$.

where $\omega = \dot{\theta}$ and parameters $L_{sk}$ are:

$$ L_{sk} = \begin{cases} L_{s0} + \dfrac{m_s}{2} M_{s0} & \text{for } k = 1 \\ L_{s0} & \text{for } k \in \{3,\, 5,\, \ldots\,, m_s - 2\} \end{cases} \quad (7) $$

Vectors ${}^{\omega}\mathbf{I}_s$ and ${}^{\omega}\mathbf{V}_s$ in (6) are defined as:

$$ {}^{\omega}\mathbf{I}_s = \Big\|\!\Big[ {}^{\omega}\mathbf{I}_{sk} \Big]\!\Big\|_{1:2:m_s-2}^{k} = \Big\|\!\Big[ \begin{smallmatrix} I_{dk} \\ I_{qk} \end{smallmatrix} \Big]\!\Big\|_{1:2:m_s-2}^{k}, \quad {}^{\omega}\mathbf{V}_s = \Big\|\!\Big[ {}^{\omega}\mathbf{V}_{sk} \Big]\!\Big\|_{1:2:m_s-2}^{k} = \Big\|\!\Big[ \begin{smallmatrix} V_{dk} \\ V_{qk} \end{smallmatrix} \Big]\!\Big\|_{1:2:m_s-2}^{k} \quad (8) $$

where $I_{dk}$, $I_{qk}$, $V_{dk}$ and $V_{qk}$ are, respectively, the *direct* and *quadrature* components of the current and voltage vectors ${}^{\omega}\mathbf{I}_s$ and ${}^{\omega}\mathbf{V}_s$. Note that using transformation ${}^{\omega}\mathbf{V}_s = {}^{t}\mathbf{T}_\omega^{\mathrm{T}}\,{}^{t}\mathbf{V}_s$ the original state space $\Sigma_t$ is transformed into $(m_s-1)/2$ two-dimensional orthogonal subspaces named $\Sigma_{\omega k}$ with $k \in \{1:2:m_s-2\}$. It can be shown, see Zanasi and Grossi (2008), that when the rotor flux function $\bar{\phi}(\theta)$ has the following structure:

$$ \bar{\phi}(\theta) = \sum_{i=1:2}^{m_s-2} a_i \cos(i\,\theta) \quad (9) $$

the torque vector ${}^{\omega}\mathbf{K}_\tau(\theta)$ is constant:

$$ {}^{\omega}\mathbf{K}_\tau = p\,\varphi_c \sqrt{\frac{m_s}{2}} \Big\|\!\Big[ \begin{smallmatrix} 0 \\ k\,a_k \end{smallmatrix} \Big]\!\Big\|_{1:2:m_s-2}^{k} = \Big\|\!\Big[ {}^{\omega}\mathbf{K}_{\tau k} \Big]\!\Big\|_{1:2:m_s-2}^{k} = \Big\|\!\Big[ \begin{smallmatrix} K_{dk} \\ K_{qk} \end{smallmatrix} \Big]\!\Big\|_{1:2:m_s-2}^{k}. \quad (10) $$

This expression clearly shows that the motor torque $\tau_m = {}^{\omega}\mathbf{K}_\tau^{\mathrm{T}}\,{}^{\omega}\mathbf{I}_s$ depends only on the *quadrature* components ${}^{\omega}I_{qk}$ of the current vector ${}^{\omega}\mathbf{I}_s$. Note that (10) holds for a generic number of phases $m_s$, while usually in the literature only a few particular cases for the torque vector ${}^{\omega}\mathbf{K}_\tau$ can be found, see for example Parsa and Toliyat (2005) and **?**. The dynamic model of a star connected multi-phase synchronous motor in the rotating frame $\Sigma_\omega$ for $m_s = 5$ is shown in Fig. 5.

### *3.2 System $\overline{S}_\omega$ in the reduced complex rotating frame $\overline{\Sigma}_\omega$*

A complex and reduced model of the multi-phase synchronous motor expressed in the rotating frame $\overline{\Sigma}_\omega$ can be obtained using the following reduced and complex pseudo-transformation matrix ${}^{t}\overline{\mathbf{T}}_{\omega N} \in \mathbb{C}^{\,m_s \times \frac{m_s-1}{2}}$:

$$ {}^{t}\overline{\mathbf{T}}_{\omega N} = {}^{t}\overline{\mathbf{T}}_\omega\,\mathbf{N}, \quad (11) $$

where ${}^{t}\overline{\mathbf{T}}_\omega$ and $\mathbf{N}$ are defined as:

$$ {}^{t}\overline{\mathbf{T}}_\omega = \sqrt{\frac{1}{m_s}} \Big\|\!\Big[ e^{jk(\theta - h\gamma_s)} \Big]\!\Big\|_{0:m_s-1 \quad 1:2:m_s-2}^{h \quad k}, \qquad \mathbf{N} = \sqrt{2}\,\mathbf{I}_{\frac{m_s-1}{2}}. \quad (12) $$

$$\left[\begin{array}{cccc|c} L_{s1} & 0 & 0 & 0 & 0 \\ 0 & L_{s1} & 0 & 0 & 0 \\ 0 & 0 & L_{s3} & 0 & 0 \\ 0 & 0 & 0 & L_{s3} & 0 \\ \hline 0 & 0 & 0 & 0 & J_m \end{array}\right]\left[\begin{array}{c} \dot{I}_{d1} \\ \dot{I}_{q1} \\ \dot{I}_{d3} \\ \dot{I}_{q3} \\ \hline \dot{\omega}_m \end{array}\right] = -\left[\begin{array}{cccc|c} R_s & -p\,\omega_m\,L_{s1} & 0 & 0 & 0 \\ p\,\omega_m\,L_{s1} & R_s & 0 & 0 & p\varphi_c\sqrt{\tfrac{5}{2}}\,a_1 \\ 0 & 0 & R_s & -3\,p\,\omega_m\,L_{s3} & 0 \\ 0 & 0 & 3\,p\,\omega_m\,L_{s3} & R_s & p\varphi_c\sqrt{\tfrac{5}{2}}\,3\,a_3 \\ \hline 0 & -p\varphi_c\sqrt{\tfrac{5}{2}}\,a_1 & 0 & -p\varphi_c\sqrt{\tfrac{5}{2}}\,3\,a_3 & b_m \end{array}\right]\left[\begin{array}{c} I_{d1} \\ I_{q1} \\ I_{d3} \\ I_{q3} \\ \hline \omega_m \end{array}\right] + \left[\begin{array}{c} V_{d1} \\ V_{q1} \\ V_{d3} \\ V_{q3} \\ \hline -\tau_e \end{array}\right]$$

Figure 5. Dynamic model of a star connected 5-phase synchronous motor in the rotating frame $\Sigma_\omega$.

$$\left[\begin{array}{cc|c} L_{s1} & 0 & 0 \\ 0 & L_{s3} & 0 \\ \hline 0 & 0 & J_m \end{array}\right]\left[\begin{array}{c} {}^{\omega}\dot{\overline{I}}_{s1} \\ {}^{\omega}\dot{\overline{I}}_{s3} \\ \hline \dot{\omega}_m \end{array}\right] = -\left[\begin{array}{cc|c} R_s + jp\,\omega_m\,L_{s1} & 0 & jp\varphi_c\sqrt{\tfrac{5}{2}}\,a_1 \\ 0 & R_s + j\,3\,p\,\omega_m\,L_{s3} & jp\varphi_c\sqrt{\tfrac{5}{2}}\,3\,a_3 \\ \hline -jp\varphi_c\sqrt{\tfrac{5}{2}}\,a_1 & -jp\varphi_c\sqrt{\tfrac{5}{2}}\,3\,a_3 & b_m \end{array}\right]\left[\begin{array}{c} {}^{\omega}\overline{I}_{s1} \\ {}^{\omega}\overline{I}_{s3} \\ \hline \omega_m \end{array}\right] + \left[\begin{array}{c} {}^{\omega}\overline{V}_{s1} \\ {}^{\omega}\overline{V}_{s3} \\ \hline -\tau_e \end{array}\right]$$

Figure 6. Dynamic model of a star connected 5-phase synchronous motor in the reduced complex rotating frame $\overline{\Sigma}_\omega$.

For a 5-phase motor the matrices ${}^{t}\overline{\mathbf{T}}_{\omega}$ and $\mathbf{N}$ are:

$${}^{t}\overline{\mathbf{T}}_{\omega} = \frac{1}{\sqrt{5}}\begin{bmatrix} e^{j\theta} & e^{j3\theta} \\ e^{j(\theta-\gamma_s)} & e^{j3(\theta-\gamma_s)} \\ e^{j(\theta-2\gamma_s)} & e^{j3(\theta-2\gamma_s)} \\ e^{j(\theta-3\gamma_s)} & e^{j3(\theta-3\gamma_s)} \\ e^{j(\theta-4\gamma_s)} & e^{j3(\theta-4\gamma_s)} \end{bmatrix}, \qquad \mathbf{N} = \begin{bmatrix} \sqrt{2} & 0 \\ 0 & \sqrt{2} \end{bmatrix}.$$

Applying the pseudo-transformation (11) to system (4), one obtains the following transformed system $\overline{S}_\omega$ expressed in the complex reduced rotating frame $\overline{\Sigma}_\omega$:

$$\left[\begin{array}{c|c} {}^{\omega}\overline{\mathbf{L}}_s & \mathbf{0} \\ \hline \mathbf{0} & J_m \end{array}\right]\left[\begin{array}{c} {}^{\omega}\dot{\overline{\mathbf{I}}}_s \\ \hline \dot{\omega}_m \end{array}\right] = -\left[\begin{array}{c|c} {}^{\omega}\overline{\mathbf{R}}_s + {}^{\omega}\overline{\mathbf{L}}_s\,{}^{\omega}\overline{\mathbf{J}}_s & {}^{\omega}\overline{\mathbf{K}}_{\tau N} \\ \hline -{}^{\omega}\overline{\mathbf{K}}^{*}_{\tau N} & b_m \end{array}\right]\left[\begin{array}{c} {}^{\omega}\overline{\mathbf{I}}_s \\ \hline \omega_m \end{array}\right] + \left[\begin{array}{c} {}^{\omega}\overline{\mathbf{V}}_s \\ \hline -\tau_e \end{array}\right] \tag{13}$$

The transformed vectors ${}^{\omega}\overline{\mathbf{I}}_s$, ${}^{\omega}\overline{\mathbf{V}}_s$ and ${}^{\omega}\overline{\mathbf{K}}_{\tau N}$ are obtained using matrix ${}^{t}\overline{\mathbf{T}}_{\omega N}$:

$${}^{\omega}\overline{\mathbf{I}}_s = {}^{t}\overline{\mathbf{T}}^{*}_{\omega N}\,{}^{t}\mathbf{I}_s = \Big\|\Big[\,{}^{\omega}\overline{I}_{sk}\,\Big]\Big\|_{1:2:m_s-2}^{k}, \quad {}^{\omega}\overline{\mathbf{V}}_s = {}^{t}\overline{\mathbf{T}}^{*}_{\omega N}\,{}^{t}\mathbf{V}_s = \Big\|\Big[\,{}^{\omega}\overline{V}_{sk}\,\Big]\Big\|_{1:2:m_s-2}^{k}$$

$${}^{\omega}\overline{\mathbf{K}}_{\tau N} = {}^{t}\overline{\mathbf{T}}^{*}_{\omega N}\,{}^{t}\mathbf{K}_{\tau} = \Big\|\Big[\,{}^{\omega}\overline{K}_{\tau k}\,\Big]\Big\|_{1:2:m_s-2}^{k} = \Big\|\Big[\,K_{dk} + jK_{qk}\,\Big]\Big\|_{1:2:m_s-2}^{k}$$

while the transformed matrices ${}^{\omega}\overline{\mathbf{L}}_s = {}^{t}\overline{\mathbf{T}}^{*}_{\omega}\,{}^{t}\mathbf{L}_s\,{}^{t}\overline{\mathbf{T}}_{\omega}$, ${}^{\omega}\overline{\mathbf{J}}_s = {}^{t}\overline{\mathbf{T}}^{*}_{\omega}\,{}^{t}\dot{\overline{\mathbf{T}}}_{\omega}$ and ${}^{\omega}\overline{\mathbf{R}}_s = {}^{t}\overline{\mathbf{T}}^{*}_{\omega}\,{}^{t}\mathbf{R}_s\,{}^{t}\overline{\mathbf{T}}_{\omega}$:

$${}^{\omega}\overline{\mathbf{L}}_s = \Big\|\Big[\,L_{sk}\,\Big]\Big\|_{1:2:m_s-2}^{k}, \quad {}^{\omega}\overline{\mathbf{J}}_s = \Big\|\Big[\,j\,kp\,\omega_m\,\Big]\Big\|_{1:2:m_s-2}^{k}, \quad {}^{\omega}\overline{\mathbf{R}}_s = R_s\mathbf{I}_{\frac{m_s-1}{2}}.$$

are obtained using the transformation matrix ${}^{t}\overline{\mathbf{T}}_{\omega}$. The components ${}^{\omega}\overline{I}_{sk}$ and ${}^{\omega}\overline{V}_{sk}$ of vectors ${}^{\omega}\overline{\mathbf{I}}_s$ and ${}^{\omega}\overline{\mathbf{V}}_s$ are complex numbers which satisfy the following relations:

$${}^{\omega}\overline{I}_{sk} = I_{dk} + jI_{qk}, \qquad {}^{\omega}\overline{V}_{sk} = V_{dk} + jV_{qk}$$

where $I_{dk}$, $I_{qk}$, $V_{dk}$ and $V_{qk}$ are the direct and quadrature components of the current and voltage vectors defined in (8). When the rotor flux function $\bar{\phi}(\theta)$ has the structure defined in (9), the torque vector ${}^{\omega}\overline{\mathbf{K}}_{\tau N}$ has a complex and constant form:

$${}^{\omega}\overline{\mathbf{K}}_{\tau N}(\theta) = {}^{\omega}\overline{\mathbf{K}}_{\tau N} = jp\varphi_c\sqrt{\frac{m_s}{2}}\,\Big\|\Big[\,ka_k\,\Big]\Big\|_{1:2:m_s-2}^{k}.$$

The original $m_s$-dimension model in the fixed frame $\Sigma_t$ has been transformed and reduced to a $(m_s-1)/2$-dimension complex model in the rotating frame $\overline{\Sigma}_\omega$. The dynamic model of a star connected multi-phase synchronous motor in the reduced complex rotating frame $\overline{\Sigma}_\omega$ for $m_s = 5$ is shown in Fig. 6. Note that the electrical part of system $\overline{S}_\omega$ has dimension $(m_s-1)/2$ while the electrical part of system $S_\omega$ has dimension $m_s-1$.

The POG scheme corresponding to the dynamic system $\overline{S}_\omega$ given in (13) is shown in Fig. 7. The function $\mathfrak{Re}(\cdot)$ present in the *connection blocks* between the power sections ①-② and ③-④ converts the transformed complex vector ${}^{\omega}\overline{\mathbf{I}}_s$ in the real vector ${}^{t}\mathbf{I}_s$:

$${}^{t}\mathbf{I}_s = \mathfrak{Re}\left({}^{t}\overline{\mathbf{T}}_{\omega N}\,{}^{\omega}\overline{\mathbf{I}}_s\right) = \mathfrak{Re}\left({}^{t}\overline{\mathbf{T}}_{\omega}\,\mathbf{N}\,{}^{\omega}\overline{\mathbf{I}}_s\right)$$

and in the real motor torque $\tau_m$:

$$\tau_m = \mathfrak{Re}\left({}^{\omega}\overline{\mathbf{K}}^{*}_{\tau N}\,{}^{\omega}\overline{\mathbf{I}}_s\right) = \mathfrak{Re}\left({}^{t}\mathbf{K}^{*}_{\tau}\,{}^{t}\overline{\mathbf{T}}_{\omega}\,\mathbf{N}\,{}^{\omega}\overline{\mathbf{I}}_s\right).$$

The mechanical part of the scheme is unchanged while the internal variables of the electrical part (between power sections ① and ③) are complex vectors of reduced dimension. Note that this transformation is *power-invariant*. Indeed it can be easily proved that the instantaneous power $p(t) = {}^{t}\mathbf{V}_s^{T}\,{}^{t}\mathbf{I}_s$ in section ① of Fig. 7 is equal to the real part of the complex instantaneous power $s(t) = {}^{\omega}\overline{\mathbf{V}}_s^{*}\,{}^{\omega}\overline{\mathbf{I}}_s$ in section ②:

$$\begin{aligned} p(t) &= {}^{t}\mathbf{V}_s^{T}\,{}^{t}\mathbf{I}_s = {}^{t}\mathbf{V}_s^{T}\,\mathfrak{Re}({}^{t}\overline{\mathbf{T}}_{\omega N}\,{}^{t}\overline{\mathbf{T}}^{*}_{\omega N})\,{}^{t}\mathbf{I}_s \\ &= \mathfrak{Re}({}^{t}\mathbf{V}_s^{T}\,{}^{t}\overline{\mathbf{T}}_{\omega N}\,{}^{t}\overline{\mathbf{T}}^{*}_{\omega N}\,{}^{t}\mathbf{I}_s) = \mathfrak{Re}({}^{\omega}\overline{\mathbf{V}}_s^{*}\,{}^{\omega}\overline{\mathbf{I}}_s) = \mathfrak{Re}(s(t)). \end{aligned}$$

Supposing the mechanical dynamics slower than the electrical one, i.e. assuming a constant velocity $\omega_m$, the eigenvalues of the following reduced system

$${}^{\omega}\overline{\mathbf{L}}_s\,{}^{\omega}\dot{\overline{\mathbf{I}}}_s = \left[{}^{\omega}\overline{\mathbf{R}}_s + {}^{\omega}\overline{\mathbf{L}}_s\,{}^{\omega}\overline{\mathbf{J}}_s\right]{}^{\omega}\overline{\mathbf{I}}_s + {}^{\omega}\overline{\mathbf{K}}_{\tau N}(\theta)\omega_m + {}^{\omega}\overline{\mathbf{V}}_s$$

are the eigenvalues of matrix $\mathbf{A} = {}^{\omega}\overline{\mathbf{L}}_s^{-1}\left[{}^{\omega}\overline{\mathbf{R}}_s + {}^{\omega}\overline{\mathbf{L}}_s\,{}^{\omega}\overline{\mathbf{J}}_s\right]$, i.e. the roots of the following polynomial $\Delta(s)$:

$$\begin{aligned} \Delta(s) &= \det\left[s\,{}^{\omega}\overline{\mathbf{L}}_s - \left({}^{\omega}\overline{\mathbf{R}}_s + {}^{\omega}\overline{\mathbf{L}}_s\,{}^{\omega}\overline{\mathbf{J}}_s\right)\right] \\ &= \det\Big\|\Big[\,sL_{sk} - R_s - j\,kp\,\omega_m L_{sk}\,\Big]\Big\|_{1:2:m_s-2}^{k} \\ &= \prod_{k}^{1:2:m_s-2}\left(sL_{sk} - R_s - j\,kp\,\omega_m L_{sk}\right) \end{aligned}$$

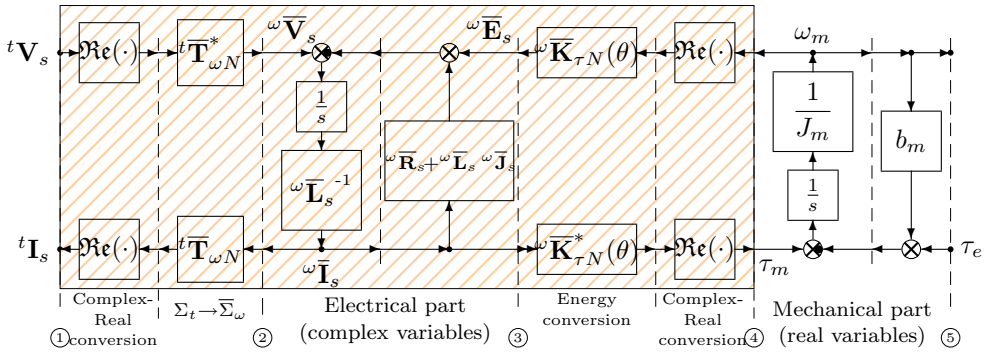


Figure 7. POG scheme of a multi-phase electrical motor in the reduced complex rotating frame $\overline{\Sigma}_\omega$.

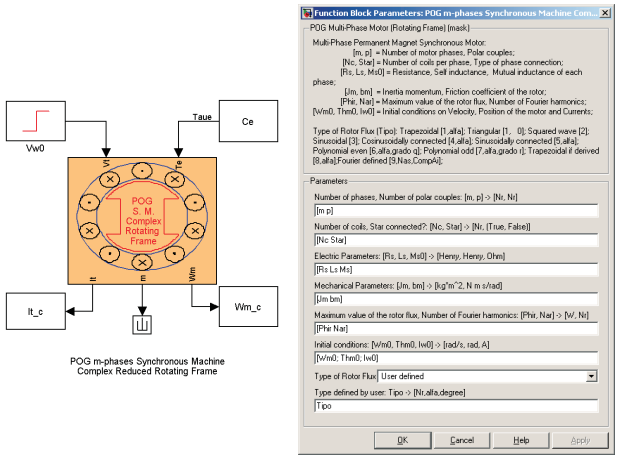


Figure 8. Simulink block scheme of the multi-phase electric motor and the corresponding user interface.

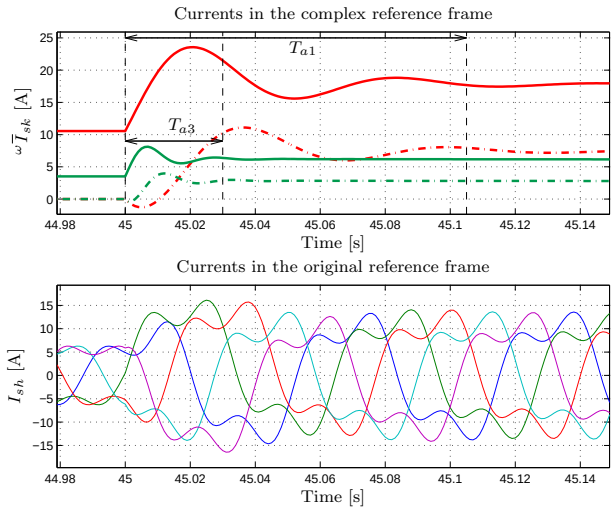


Figure 9. Currents in the $\overline{\Sigma}_\omega$ and $\Sigma_t$ reference frames.

Note that the characteristic polynomial $\Delta(s)$ has complex coefficients and therefore its $(m_s-1)/2$ roots are not necessarily complex conjugate. In this case the roots of polynomial $\Delta(s)$ can be easily found because ${}^{\omega}\overline{\mathbf{L}}_s$, ${}^{\omega}\overline{\mathbf{R}}_s$ and ${}^{\omega}\overline{\mathbf{J}}_s$ are block diagonal matrices. The $(m_s-1)/2$ roots $\lambda_k$ of $\Delta(s)$ are:

$$\lambda_k = \frac{R_s}{L_{sk}} + j\,kp\,\omega_m \qquad \text{for} \qquad k = 1:2:m_s-2 \tag{14}$$

and the corresponding settling times $T_{ak}$ are:

$$T_{ak} = \frac{3}{|\mathrm{Re}(\lambda_k)|} \qquad \text{for} \qquad k = 1:2:m_s-2 \tag{15}$$

For the transformed system $\overline{S}_\omega$ obtained using the state space transformation (11) the following property holds: when $\omega_n$ is constant, the $m_s-1$ eigenvalues of the considered multi-phase synchronous motor coincide with the $(m_s-1)/2$ eigenvalues of system $\overline{S}_\omega$, i.e. the complex roots (14) of polynomial $\Delta(s)$, and their $(m_s-1)/2$ complex conjugate values.

## 4. SIMULATION

The dynamic models of the multi-phase electric motor shown in Fig. 4 and in Fig. 7 have been implemented in Simulink. The Simulink block scheme of the dynamic model of Fig. 7 and the corresponding user interface are shown in Fig. 8. A very important advantage of exploiting the POG technique with vectorial notation is that the Simulink scheme is very compact and there is no need to consider separate fictitious machines. With this approach a unique general model is used whatever the number of phases $m_s$ is. Thanks to the graphical interface shown in Fig. 8, the user can modify the number of phases and the parameters of the model without changing the structure of the model.

The simulation results shown in Fig. 9 and Fig. 10 have been obtained using the following electrical and mechanical parameters: $m_s = 5$, $p = 1$, $R_s = 1.5\,\Omega$, $L_s = 0.03$ H, $M_{s0} = 0.015$ H, $\varphi_r = 0.02$ Wb, $J_m = 1.5$ kg m$^2$, $b_m = 0.1$ Nm s/rad, $V_{max} = 100$ V, $a_1 = 0.9$, $a_3 = 0.1$ and the external torque $\tau_e = 0$ Nm. The system has been fed with the following input, see the POG scheme of Fig. 7:

$${}^{\omega}\overline{\mathbf{V}}_{s0} = ({}^{\omega}\overline{\mathbf{R}}_s + {}^{\omega}\overline{\mathbf{J}}_s\,{}^{\omega}\overline{\mathbf{L}}_s)\,{}^{\omega}\overline{\mathbf{I}}_d + {}^{\omega}\overline{\mathbf{K}}_\tau\,\omega_{md}$$

where ${}^{\omega}\overline{\mathbf{I}}_d$ and $\omega_{md}$ are the desired current vector and motor velocity, respectively. The desired current vector ${}^{\omega}\overline{\mathbf{I}}_d$ that provide the desired torque $\tau_d$ minimizing the current dissipation is the current vector parallel to the torque vector ${}^{\omega}\overline{\mathbf{K}}_{\tau N}$:

$${}^{\omega}\overline{\mathbf{I}}_d = \frac{{}^{\omega}\overline{\mathbf{K}}_{\tau N}}{|{}^{\omega}\overline{\mathbf{K}}_{\tau N}|^2}\,\tau_d = \Big[\!\Big[\, j\tau_d \underset{1:2:m_s-2}{\overset{k}{\widetilde{K}_k}} \,\Big]\!\Big], \quad \widetilde{K}_k = \frac{K_{qk}}{|{}^{\omega}\mathbf{K}_{\tau N}|^2}$$

The desired torque is $\tau_d = 10$ Nm for $t \in [0, 45[$ s and $\tau_d = 15$ Nm for $t \geq 45$ s therefore at $t = 45\,s$ a step is applied to voltage vector ${}^{\omega}\overline{\mathbf{V}}_{s0}$ to see the open-loop step response of the system. The time behaviors of stator currents ${}^{t}\mathbf{I}_s$ and ${}^{\omega}\overline{\mathbf{I}}_s$ in frames $\Sigma_t$ and $\overline{\Sigma}_\omega$ are shown in Fig. 9. The transient of the components ${}^{\omega}\overline{I}_{sk}$ of vector ${}^{\omega}\overline{\mathbf{I}}_s$ is deeply related to the poles (14) of the electrical part

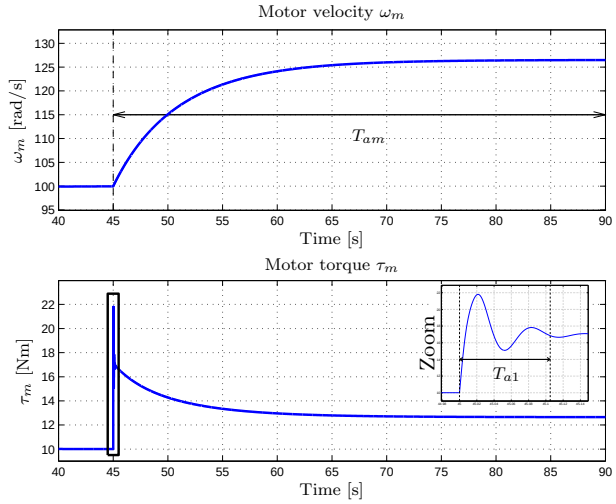


Figure 10. Motor velocity $\omega_m$ and motor torque $\tau_m$.

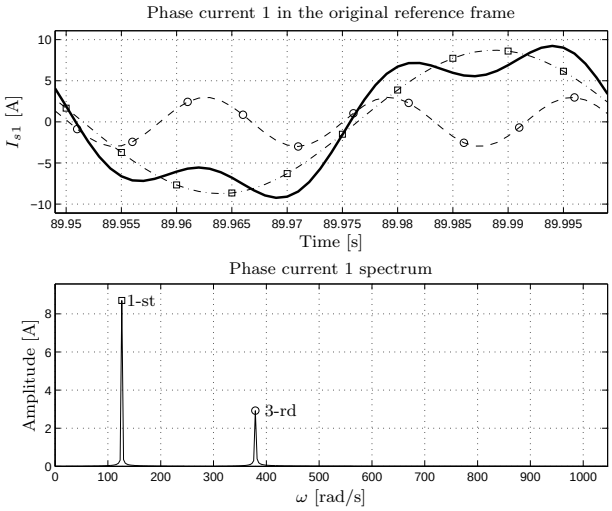


Figure 11. Phase current 1 waveform and harmonic spectrum in steady-state condition.

of the system: $\lambda_1 = -28.6 \pm j\,100$ and $\lambda_3 = -100 \pm j\,300$ when $\omega_m = 100$ rad/s. The corresponding settling times $T_{ak}$ obtained using (15) are:

$$T_{a1} = \frac{3}{|\mathrm{Re}(\lambda_1)|} \approx 0.11 \text{ s}, \qquad T_{a3} = \frac{3}{|\mathrm{Re}(\lambda_3)|} \approx 0.03 \text{ s}.$$

The time behaviors of motor velocity $\omega_m$ and motor torque $\tau_m$ are shown in Fig. 10. The torque transient is deeply related to the electrical dominant poles of the system located in $\lambda_1$, while the motor velocity transient is related to the mechanical pole located in $\lambda_m = -b_m/J_m = -0.067$. The mechanical settling time is:

$$T_{am} = \frac{3}{|\mathrm{Re}(\lambda_m)|} \approx 45 \text{ s}.$$

For $t > T_{a1}$ the torque variation is mainly due to the increasing of motor velocity which causes the variation of back-emf. Since the components ${}^{\omega}\overline{I}_{s1}$ and ${}^{\omega}\overline{I}_{s3}$ of vector ${}^{\omega}\overline{\mathbf{I}}_s$ are both different from zero, then the harmonic spectrum of the phase current waveform contains the 1-st and the 3-rd harmonics, as it is shown in Fig. 11. The same simulation results have been obtained also using the Simulink implementation of the POG scheme of Fig. 4 which describes the multi-phase electric motor with respect to the rotating frame $\Sigma_\omega$: the order of the error between the two simulations is $10^{-14}$.

## 5. CONCLUSION

In this paper the modeling of multi-phase synchronous motors with an odd number of phases has been investigated with a specific focus on the coordinate transformations which allows to write the system dynamics in a compact and reduced form. Two state space transformations (one real and one complex) have been presented. The proposed transformations have some advantages with respect to those used in the literature: they are *power-invariant* and they use a very compact vectorial notation. The POG schemes used to represent the considered models has the important advantage that they can be directly implemented in Simulink and therefore there is no need to consider separate fictitious machines. The presented simulation results have shown the effectiveness and the precision of the proposed transformations.

## REFERENCES


D. C. White and H. H. Woodson, "Electromechanical Energy Conversion." New York: Wiley, 1959

Parsa, L. and Toliyat, H.A., "Five-Phase Permanent-Magnet Motor Drives", IEEE Transactions on Industry Applications, 2005, Vol. 41, No. 1, pp. 30-37.

X. Kestelyn, E. Semail, JP. Hautier, "Vectorial Multi-machine Modeling for a Five-Phase Machine", in Proc. Int. Conf. Electrical Machines (ICEM), Bruges, Belgium, 2002, CD-ROM, Paper 394.

E. Semail, X. Kestelyn, A. Bouscayrol, "Right Harmonic Spectrum for the Back-Electromotive Force of a $n$-phase Synchronous Motor", Industry Applications Conference, 2004, 39th IAS Annual Meeting, ISBN: 0-7803-8486-5.

Paap, G.C., "Symmetrical Components in the Time Domain and Their Application to Power Network Calculations", IEEE Transactions on Power Systems, Volume 15, Issue 2, pp.522-528, 2000.

C. L. Fortescue, "Method of Symmetrical Coordinates Applied to the Solution of Polyphase Networks." Trans. AIEE, pt. II, vol. 37, pp.1027-1140, 1918

Grandi G.; Serra G.; Tani A., "General Analysis of Multi-Phase Systems Based on Space Vector Approach", Power Electronics and Motion Control Conference, EPE-PEMC 2006, pp.834-840

E.Clarke, "Circuit Analysis of AC Power System." New York: Wiley, 1950, vol.I

R. H. Park, "Two-reaction theory of synchronous machines." Trans. AIEE , vol. 48, pp. 716, 1929.

R. Zanasi, F. Grossi "Optimal Rotor Flux Shape for Multi-phase Permanent Magnet Synchronous Motors", International Power Electronics and Motion Control Conference, 2008, Poznan, Poland.

R. Zanasi, "Power Oriented Modelling of Dynamical System for Simulation", IMACS Symp. on Modelling and Control of Technological System, Lille, France, 1991.

R. Zanasi, "The Power-Oriented Graphs Technique: system modeling and basic properties", Vehicular Power and Propulsion Conference, Lille, France, Sept 2010.

R. Zanasi, F. Grossi. *Vectorial Control of Multi-phase Synchronous Motors using POG Approach.* IECON 2009, 35th Annual Conference of the IEEE Industrial Electronics Society, 2009 Porto, Portugal.